Research Article

An Effective Method for Electromagnetic Parameter Measurement of Flexible Materials Based on Air Coaxial Line

Jinjing Ren ⓘ**, Mingjie Sheng** ⓘ**, and Zhongyuan Zhou** ⓘ

Research Center for Electromagnetic Environment Effects, Southeast University, Nanjing 211189, China

Correspondence should be addressed to Mingjie Sheng; smj@seu.edu.cn and Zhongyuan Zhou; zyzhou@seu.edu.cn

When measuring the electromagnetic parameters of flexible material with an air coaxial line, the specimen is prone to bend and deform in the fixture, which results in erroneous results. In order to solve this problem, this paper proposes a new measurement method. Firstly, a rigid material is selected and loaded into the air coaxial line for two-port *S* parameters measurement. Then, the flexible material is attached to one end of the rigid material and loaded into the air coaxial line together for repeated two-port *S* parameter measurement. According to the *S* parameters measured and the two-port network cascading theory, the *S* parameters of the flexible material separately loaded in the fixture can be deduced. Finally, the electromagnetic parameters of the flexible material can be calculated by the Nicolson–Ross–Weir (NRW) method. Experimental results show that the method proposed is effective and reliable.

1. Introduction

The electromagnetic parameters of materials mainly include complex permittivity and complex permeability [1, 2]. The commonly used measurement methods include lumped parameter, network parameter, and resonant cavity method [3–5]. The network parameter method based on air coaxial line is widely used because of its wide band and simple operation [6]. The measurement setup with an air coaxial line is shown in Figure 1. The specimen must be made into a concentric circle with the same section size as the device (specimen 1 in Figure 1) and loaded into the air coaxial line for two-port *S* parameters measurement. Conversion methods can obtain the electromagnetic parameters of the material according to the *S* parameters measured. There are many kinds of conversion methods based on the air coaxial line. The standard ASTM D7449 [7] summarizes and compares their characteristics. The NRW method only needs the reflection and transmission coefficients and can calculate both the complex permittivity and complex permeability, which the standard recommends [7–9]. The measurement process is easy to implement for materials with good rigidity [10]. However, for thin flexible materials, bending and

deformations are prone to occur during clamping, as specimens 2 and 3 in Figure 1, which will result in inaccurate measurement results.

To avoid this problem, a waveguide can be adopted as the measurement device, but the working frequency of it is narrow [11–13]. Another approach is sticking multiple pieces of specimens together to increase the material's rigidity by increasing the thickness. However, many adhesives will be introduced, which will lead to a deviation between the test results and the real electromagnetic parameters of the material. Reference [14] proposes a method to determine the dielectric model parameters of thin-film material with an air coaxial line. The method is based on input impedance measurement and calculates the electromagnetic parameters in the low frequency band. For higher frequencies, the method does not work because of the resonance.

This paper proposes a measurement method for attaching flexible material to rigid material. Firstly, we select a rigid material with a smooth end face as the substrate and load it into the air coaxial line to measure the two-port *S* parameters. Then, we attach the flexible material to one end of the substrate and load these two materials into the air coaxial line together to measure the two-port *S* parameters
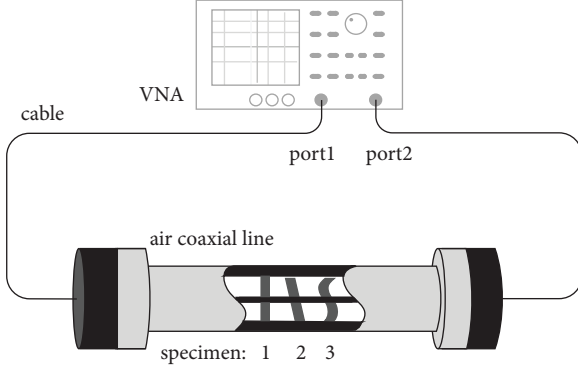
FIGURE 1: Setup for electromagnetic parameter measurement with an air coaxial line.

FIGURE 2: The cross section of the air coaxial line containing a specimen.

again. The results can be regarded as a cascade of two two-port networks. According to the S parameters measured above and the transition matrix of cascaded networks, the S parameters of the flexible material separately and flatly loaded in the air coaxial line can be calculated. Finally, the complex permittivity and permeability can be obtained with the NRW method. In the process mentioned above, the substrate material should be put at the same position in the air coaxial line, which is very important.

2. Methods and Principle

2.1. Measurement Method and Procedure.

The cross section of the air coaxial line with a rigid material specimen is shown in Figure 2. The standard [7] gives the calculation equations of complex permittivity and complex permeability based on the NRW method as follows:

$$\mu_r = \frac{2\pi}{\Lambda\sqrt{\gamma_0{}^2 - \gamma_c{}^2}}\left(\frac{1+\Gamma}{1-\Gamma}\right), \tag{1}$$

$$\varepsilon_r = \frac{2\pi}{\mu_r\gamma_0^2}\left(\frac{4\pi^2}{\Lambda^2} = \gamma_c^2\right), \tag{2}$$

where $\Gamma = X \pm \sqrt{X^2 - 1}$, $X = S_{11}^2 - S_{21}^2 + 1/2S_{11}$, $T = S_{11} + S_{21} - \Gamma/1 - (S_{11} + S_{21})\Gamma$, $1/\Lambda^2 = -[1/2\pi L \in (T)]^2$, $\gamma_0 = j2\pi f \sqrt{\varepsilon_0\mu_0}$ is the propagation constant of the air section, and $\gamma_c = \gamma_0\sqrt{\varepsilon_r\mu_r}$ is the propagation constant of the specimen section. The references of S_{11} and S_{21} are planes 2 and 3, respectively. It can be seen from equations (1) and (2) that in order to calculate the complex permittivity and complex permeability, getting values of the reflection coefficient and transmission coefficient at both ends of the specimen is the prerequisite.

In the NRW method, it is necessary to know the position of the specimen in the air coaxial line accurately when measuring the electromagnetic parameters of materials [9]. For the convenience of measurement, the end face of the specimen is generally flush with one port of the fixture, i.e., l_1 or l_2 is equal to 0 in Figure 2. It is difficult to ensure that the substrate is always at the same position in
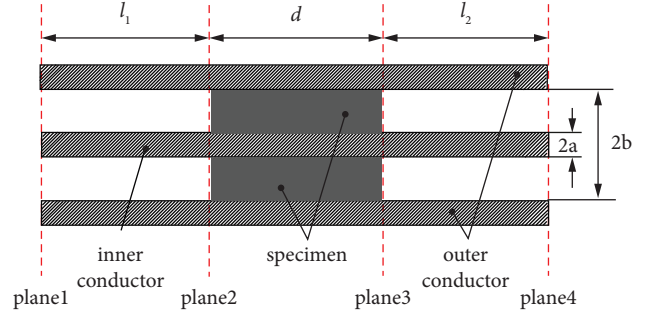
the air coaxial line during multiple measurements. In order to make the measurement more operable, the measurement process proposed in this paper is shown in Figure 3, where Z_0, Z_1, Z_2, and Z_3 are the characteristic impedances of the air, specimen 1, specimen 2, and specimen 3 sections in the air coaxial line, respectively, and the specimens 1 and 2 are the same material in this paper, i.e., $Z_1 = Z_2$. The measurement process is as follows: first, we load the rigid material specimens 1 and 2 into the air coaxial line from port 1 in sequence as shown in Figure 3(a) and measure the S parameters between planes 1 and 4 with the vector network analyzer (VNA). Because the specimen and the inner conductor of the air coaxial line are tightly matched and the end faces of specimens 1 and 2 are smooth, it can be considered that there is no air gap between specimens. In this case, the S parameters measured can be regarded as the results of the two-port network cascade of specimens 1 and 2. Then, we put specimen 2 into the air coaxial line separately as shown in Figure 3(b) and measure the S parameters. Finally, we load specimen 1 and the material to be tested (specimen 3) into the air coaxial line in sequence and measure the S parameters between planes 1 and 4 again. The results can be regarded as the two-port network cascading of specimens 1 and 3. According to the process mentioned above, S parameters of specimen 3 separately loaded into the air coaxial line (as shown in Figure 3(d)) can be deduced. It is noted that the thickness of specimens 2 and 3 should be the same.

2.2. Calculation and Principle.

To express clearly, $[T]_{(n,k)(i,j)}$ and $S_{xy(i,j)}$ are used to represent the transmission matrix and the S parameters in calculations, respectively, and S_{xym} is used to represent the S parameters obtained from VNA, where n and k represent the measurement specimen, respectively, and i and j represent the reference plane. The scattering matrix of the equivalent two-port network can be obtained from measurements in Figures 3(a)–3(c) directly. For the cascaded two-port network, the transfer matrix is adopted for analysis [15].

We suppose that the transfer matrix is expressed as equation (3) when the characteristic impedance on both sides of the specimen I is Z_0.
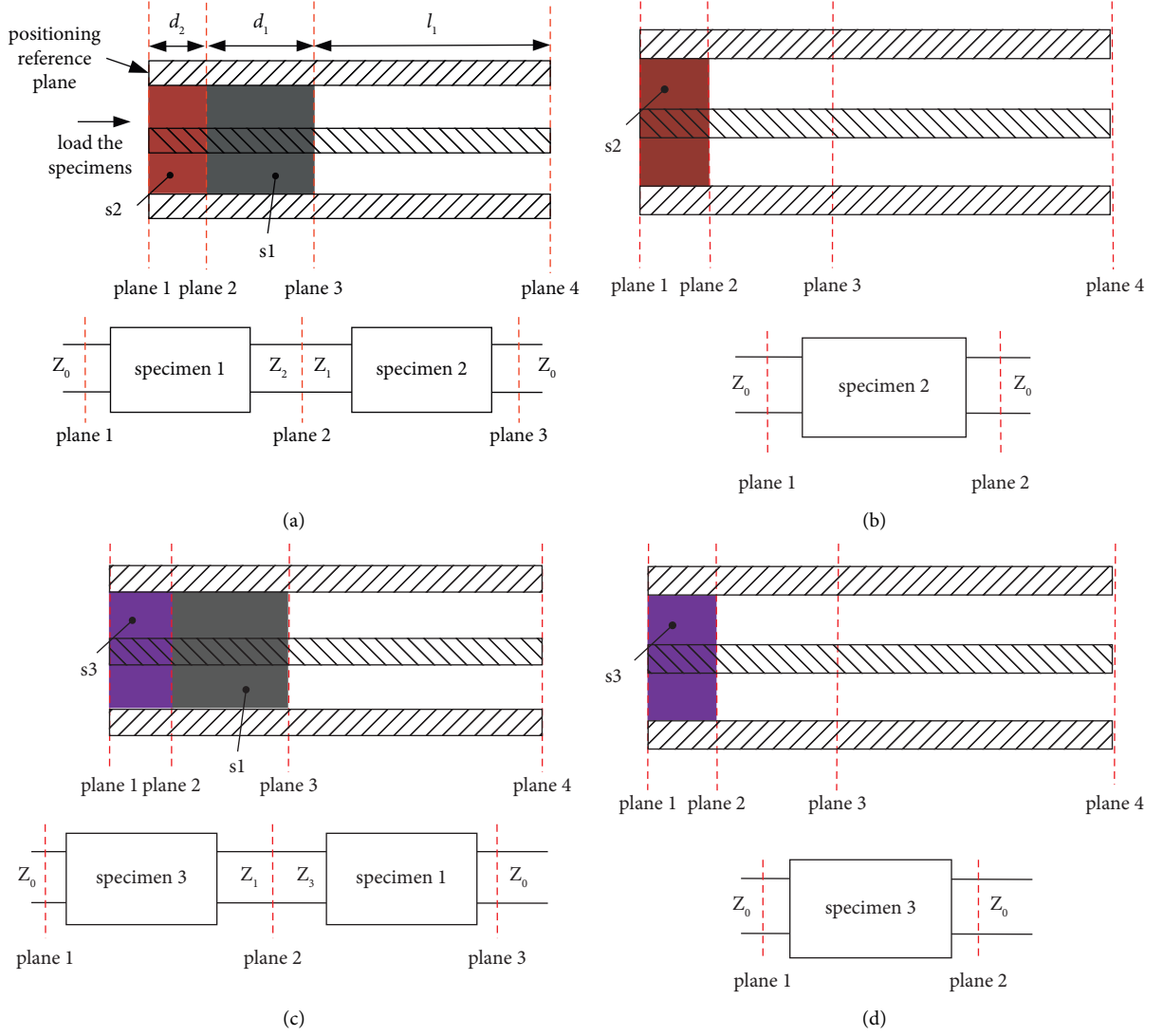
FIGURE 3: Measurement process of electromagnetic parameters of flexible materials. (a) Step 1: measurement and equivalent network of specimens 1 and 2. (b) Step 2: measurement and equivalent network of specimen 2. (c) Step 3: measurement and equivalent network of specimens 1 and 3. (d) Equivalent measurement of specimens 3 derived from step 1, step 2, and step 3.

$$[T]_i = \begin{bmatrix} a_i & Z_0 b_i \\ \dfrac{1}{Z_0}c_i & d_i \end{bmatrix}. \tag{3}$$

The corresponding normalized transfer matrix is expressed as [15]

$$[\tilde{T}]_i = \begin{bmatrix} a_i & b_i \\ c_i & d_i \end{bmatrix}, \tag{4}$$

where $i = 1$, 2, or 3 and a, b, c, and d are the four elements of the normalized transition matrix $[\tilde{T}]$ [16].

2.2.1. For Measurement in Figure 3(a).
The transfer matrices of specimens 1 and 2 are expressed as equations (5) and (6), respectively.

$$[T]_{(1)(2,3)} = \begin{bmatrix} \sqrt{\dfrac{Z_2}{Z_0}}a_1 & \sqrt{Z_0 Z_2}\, b_1 \\ \dfrac{1}{\sqrt{Z_0 Z_2}}c_1 & \sqrt{\dfrac{Z_0}{Z_2}}d_1 \end{bmatrix}, \tag{5}$$

$$[T]_{(2)(1,2)} = \begin{bmatrix} \sqrt{\dfrac{Z_0}{Z_1}}a_2 & \sqrt{Z_0 Z_1}\, b_2 \\ \dfrac{1}{\sqrt{Z_0 Z_1}}c_2 & \sqrt{\dfrac{Z_1}{Z_0}}d_2 \end{bmatrix}. \tag{6}$$

According to the two-port network cascade theory, the transition matrix of the cascaded networks is equal to the product of single network transition matrix. So, for the measurements in Figure 3(a), we can get

$$[T]_{(2,1)(1,3)} = [T]_{(2)(1,2)}[T]_{(1)(2,3)} = \begin{bmatrix} a_1a_2 + b_2c_1 & Z_0(b_1a_2 + b_2d_1) \\ \dfrac{1}{Z_0}(a_1c_2 + c_1d_2) & b_1c_2 + d_1d_2 \end{bmatrix}, \tag{7}$$

where $[T]_{(2,1)(1,3)}$ can be deduced from the S parameters measured as [15]

$$[T]_{(2,1)(1,3)} = \frac{1}{2S_{21(1,3)}}\begin{bmatrix} A_1 & B_1 \\ C_1 & D_1 \end{bmatrix}, \tag{8}$$

where

$$\begin{cases} A_1 = (1 + S_{11(1)})(1 - S_{22(3)}) + S_{12(1,3)}S_{21(1,3)}, \\[2mm] B_1 = Z_0((1 + S_{11(1)})(1 + S_{22(3)}) - S_{12(1,3)}S_{21(1,3)}), \\[2mm] C_1 = \frac{1}{Z_0}((1 - S_{11(1)})(1 - S_{22(2)}) - S_{12(1,3)}S_{21(1,3)}), \\[2mm] D_1 = (1 - S_{11(1)})(1 + S_{22(3)}) + S_{12(1,3)}S_{21(1,3)}. \end{cases} \tag{9}$$

The reference planes of S parameters directly measured by VNA are planes 1 and 4, so it is necessary to convert the reference planes as

$$\begin{cases} S_{11(1)} = S_{11m}, & S_{11(2)} = S_{11m}e^{2\gamma_0 d_2}, \\[1mm] S_{21(1,3)} = S_{21m}e^{\gamma_0 l_1}, & S_{21(1,2)} = S_{21m}e^{\gamma_0 (l_1+d_1)}, \\[1mm] S_{21(1,3)} = S_{12m}e^{\gamma_0 l_1}, & S_{12(1,2)} = S_{12m}e^{\gamma_0 (l_1+d_1)}, \\[1mm] S_{22(2)} = S_{22m}e^{2\gamma_0 (l_1+d_1)}, & S_{22(3)} = S_{22m}e^{2\gamma_0 l_1}. \end{cases} \tag{10}$$

Based on equations (7) to (10), the product of $[\tilde{T}]_2$ and $[\tilde{T}]_1$ can be calculated.

2.2.2. For Measurement in Figure 3(b)

$$[T]_{(2)(1,2)} = \begin{bmatrix} a_2 & Z_0b_2 \\ Z_0c_2 & d_2 \end{bmatrix} = \frac{1}{2S_{21(1,2)}}\begin{bmatrix} A_2 & B_2 \\ C_2 & D_2 \end{bmatrix}, \tag{11}$$

where

$$\begin{cases} A_2 = (1 + S_{11(1)})(1 - S_{22(2)}) + S_{12(1,2)}S_{21(1,2)}, \\[2mm] B_2 = Z_0((1 + S_{11(1)})(1 + S_{22(2)}) - S_{12(1,2)}S_{21(1,2)}), \\[2mm] C_2 = \frac{1}{Z_0}((1 - S_{11(1)})(1 - S_{22(2)}) - S_{12(1,2)}S_{21(1,2)}), \\[2mm] D_2 = (1 - S_{11(1)})(1 + S_{22(2)}) + S_{12(1,2)}S_{21(1,2)}. \end{cases} \tag{12}$$

$[\tilde{T}]_2$ can be solved from equations (11) and (12) Combined with the results obtained from measurement in Figure 3(a), $[\tilde{T}]_1$ can be calculated.

2.2.3. For Measurement in Figure 3(c)

$$[T]_{(3,1)(1,3)} = [T]_{(3)(1,2)}[T]_{(1)(2,3)} = \begin{bmatrix} Za_1a_3 + \dfrac{1}{Z}b_3c_1 & Z_0\left(Za_3b_1 + \dfrac{1}{Z}b_3d_1\right) \\ \dfrac{1}{Z_0}\left(Za_1c_3 + \dfrac{1}{Z}c_1d_3\right) & Zb_1c_3 + \dfrac{1}{Z}d_1d_3 \end{bmatrix} = \frac{1}{2S_{21(1,3)}}\begin{bmatrix} A_3 & B_3 \\ C_3 & D_3 \end{bmatrix}, \tag{13}$$

where

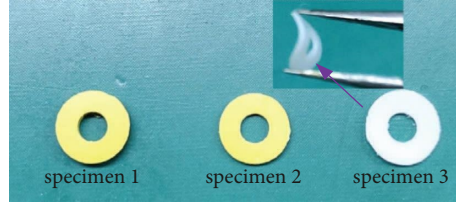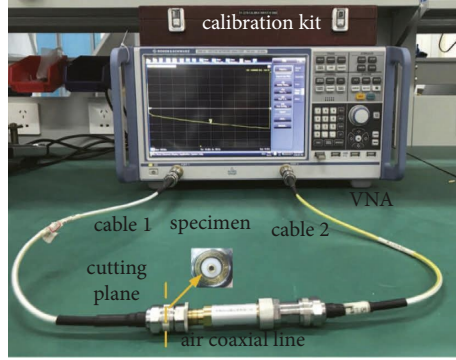FIGURE 4: Photo of specimens.

FIGURE 5: Measurement setup.

$$\begin{cases} A_3 = \left(1 + S_{11(1)}\right)\left(1 - S_{22(3)}\right) + S_{12(1,3)}S_{21(1,3)}, \\[2mm] B_3 = Z_0\left(\left(1 + S_{11(1)}\right)\left(1 + S_{22(3)}\right) - S_{12(1,3)}S_{21(1,3)}\right), \\[2mm] C_3 = \dfrac{1}{Z_0}\left(\left(1 - S_{11(1)}\right)\left(1 - S_{22(3)}\right) - S_{12(1,3)}S_{21(1,3)}\right), \\[2mm] D_3 = \left(1 - S_{11(1)}\right)\left(1 + S_{22(3)}\right) + S_{12(1,3)}S_{21(1,3)}, \\[2mm] Z = \sqrt{\dfrac{Z_3}{Z_1}}. \end{cases} \quad (14)$$

For the convenience of calculation, we decompose equations (13) as

$$[T]_{(3,1)(1,3)} = \begin{bmatrix} Za_3 & Z_0\dfrac{1}{Z}b_3 \\[2mm] \dfrac{Z}{Z_0}c_3 & \dfrac{1}{Z}d_3 \end{bmatrix} \begin{bmatrix} a_1 & Z_0b_1 \\[2mm] \dfrac{1}{Z_0}c_1 & d_1 \end{bmatrix} = \begin{bmatrix} Za_3 & Z_0\dfrac{1}{Z}b_3 \\[2mm] \dfrac{Z}{Z_0}c_3 & \dfrac{1}{Z}d_3 \end{bmatrix}[T]_1. \quad (15)$$

In (15), $[T]_{(3,1)(1,3)}$ and $[T]_1$ are already calculated, so we can get the following:

$$\begin{bmatrix} Za_3 & Z_0Zb_3 \\[2mm] \dfrac{1}{ZZ_0}c_3 & \dfrac{1}{Z}d_3 \end{bmatrix} = [T]_{(3,1)(1,3)}[T]_1^{-1}. \quad (16)$$

The two-port network corresponding to $[T]_3$ is symmetric, and equation (17) can be obtained according to its properties [16].

$$a_3 = d_3. \quad (17)$$

Now, there are four unknowns $(a_3(d_3), b_3, c_3, \text{and } Z)$ and four equations in equation (16), so $[T]_3$ and $[\widetilde{T}]_3$ can be solved easily. According to the transformation relationship between the scattering parameters and the transfer matrix [16], S parameters of the two-port network in Figure 3(d) can be obtained. Finally, the electromagnetic parameters of specimen 3 can be calculated by the NRW method (Equations (1) and (2)).

2.3. Experiment and Analysis. In this part, flexible material is measured. A piece of polytetrafluoroethylene (PTFE) with the thickness of 0.5 mm shown in Figure 4 is adopted as specimen 3 to carry out the verification experiment. The electromagnetic parameters are obtained with the method proposed in this paper, which are compared with the reference values. The reference values are obtained from the measurement with the air coaxial line according to the standard [7], where a 2 mm PTFE specimen is adopted. For specimens 1 and 2, rigid materials code K04 with the thickness of 2 mm and 0.5 mm are selected, respectively. The inner and outer diameters of specimens all meet the test requirements of the air coaxial line, which are shown in Figure 4.

The measurement setup is shown in Figure 5, where the VNA is R&S ZNB20 and is calibrated by the calibration kit R&S ZVZ270 (type N, 50 Ω). The settings are as follows: frequency 0.1 GHz to 18 GHz, output power −10 dBm, IF bandwidth 700 Hz, 1601 sampling points, and no averaging
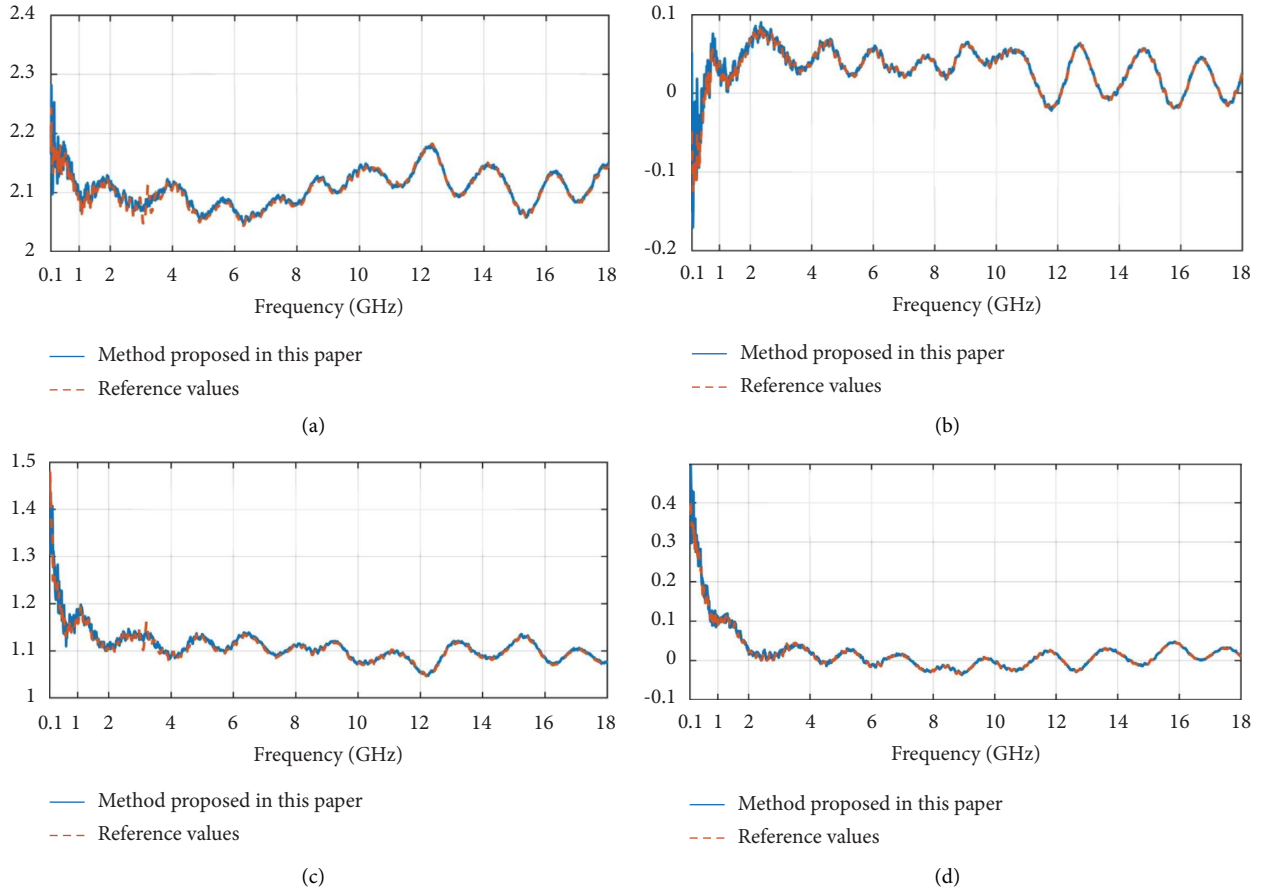
FIGURE 6: Comparison between measurement results and reference values (the measurement results in blue are based on the proposed method in this paper and the reference values in red are based on the method in standard ASTM D7449): (a) real part of relative permittivity, (b) imaginary part of relative permittivity, (c) real part of relative permeability, and (d) imaginary part of permeability.

applied to data. The outer diameter of the air coaxial line is 7.0 mm, the diameter of the inner conductor is 3.04 mm, and the length is 80 mm.

The results are shown in Figure 6. The measurement results in blue are based on the proposed method in this paper and the reference values in red are based on the method in standard ASTM D7449. It can be seen that the results of the method proposed in this paper consist well with the reference value from 1 GHz to 18 GHz. It proves the effectiveness of the method proposed. At low frequencies (0.1 GHz ~ 1 GHz), the curves of the method proposed show larger fluctuations. This is because the measurement with VNA shows greater uncertainty when the thickness of the specimen is only 0.5 mm [17]. It should be noted that the thickness of the substrate (specimen 1) in this paper should be chosen carefully to avoid resonance [18].

3. Conclusions

A method for the electromagnetic parameters measurement of flexible materials based on air coaxial line is proposed in this paper. The method solves the problem that the specimen is easy to deform in the process of

installation when measuring the electromagnetic parameters of flexible materials with the air coaxial line. The experimental results show that the proposed method is effective and feasible.

In order to obtain the transfer matrix of specimen 1 in step 3, measurement procedure steps 1 and 2 are introduced. Actually, there are also some other solutions. For example, specimen 1 can be loaded at one certain position of the air coaxial line for S parameters measurement, and the transfer matrix can be calculated by phase extension then. However, the procedure in this paper is more maneuverable in engineering. It is also possible to fix the flexible specimen further by using two rigid specimens based on the method in this paper.

Data Availability

The data used to support the findings of this study are included within the article.

Conflicts of Interest

The authors declare that they have no conflicts of interest.

Acknowledgments

References

[1] L. Solymar and D. Walsh, *Electrical Properties of Materials*, Oxford University Press, Oxford, UK, 1998.

[2] X. C. Tong, *Advanced Materials and Design for Electromagnetic Interference Shielding*, CRC Press, Boca Raton, FL, USA, 2008.

[3] J. C. E. Sten and P. K. Koivisto, "Determining both the permittivity and the permeability of small samples using cavity perturbation method," *Measurement Science and Technology*, vol. 20, no. 5, pp. 057001–057122, 2009.

[4] J. Sheen, "Measurements of microwave dielectric properties by an amended cavity perturbation technique," *Measurement*, vol. 42, no. 1, pp. 57–61, 2009.

[5] H. Lu, S. Jing, T. Xia, J. Yang, Z. Yin, and G. Deng, "Measurement of lc dielectric constant at lower terahertz region based on metamaterial absorber," *IEICE Electronics Express*, vol. 14, no. 12, Article ID 20170469, 2017.

[6] C. Guoxin, "Calibration-independent measurement of complex permittivity of liquids using a coaxial transmission line," *Review of Scientific Instruments*, vol. 86, no. 1, Article ID 014704, 2015.

[7] ASTM D7449, *Standard Test Method for Measuring Relative Complex Permittivity and Relative Magnetic Permeability of Solid Materials at Microwave Frequencies Using Coaxial Air Line*, American Society for Testing Materials, West Conshohocken, PA, USA, 2014.

[8] J. Baker-Jarvis, M. Janezic, J. H. Grosvenor, and R. G. Geyer, "Transmission/reflection and short-circuit line methods for measuring permittivity and permeability," *NIST Technical Note*, vol. 1536, 2004.

[9] H. Wang, J. Shan, G. Wang, and X. Ke, "Electromagnetic parameters test system based on a refined NRW transmission/reflection algorithm," in *Proceedings of the International Symposium on Microwave*, Hangzhou, China, August 2007.

[10] E. Georget, F. Diaby, R. Abdeddaim, and P. Sabouroux, "Permittivity measurement of materials of different natures," in *Proceedings of the 8th European Conference on Antennas and Propagation (EuCAP 2014)*, Hague, Netherlands, April 2014.

[11] R. A. Alahnomi, Z. Zakaria, E. Ruslan, and A. A. M. Bahar, "A novel symmetrical split ring resonator based on microstrip for microwave sensors," *Measurement Science Review*, vol. 16, no. 1, pp. 21–27, 2016.

[12] ASTM D5568, *Standard Test Method for Measuring Relative Complex Permittivity and Relative Magnetic Permeability of Solid Materials at Microwave Frequencies Using Waveguide*, American Society for Testing Materials, West Conshohocken, PA, USA, 2008.

[13] A. Kik and A. Nishikata, "Analysis of errors in permittivity measurements using the waveguide-penetration method," *IEICE - Transactions on Communications*, vol. E93, no. 7, pp. 1697–1706, 2010.

[14] M. Sheng, Z. Zhou, Y. Gu, Q. Zhou, Y. Xiao, and F. Tian, "A measurement method for electromagnetic parameters of flexible materials in low frequency band," in *Proceedings of the 2021 Asia-Pacific International Symposium on Electromagnetic Compatibility (APEMC)*, Bali, Indonesia, September 2021.

[15] D. M. Pozar, *Microwave Engineering*, Publishing House of Electronics Industry, Beijing, China, 2011.

[16] X. Zhou, *Basis of Electromagnetic Field Theory and Microwave Technology*, Southeast University Press, Nanjing, China, 2010.

[17] Agilent Application Note, *Agilent Basics of Measuring the Dielectric Properties of Materials*, 2014, http://www.agilent.com.

[18] Y. Huang, *Electromagnetic fields and Microwave Technique*, Post & Telecom Press, Beijing, China, 2012.